Developmental Biology 336 (2009) 232–245

Contents lists available at ScienceDirect

Developmental Biology

journal homepage: www.elsevier.com/developmentalbiology

FoxD5 mediates anterior–posterior polarity through upstream modulator Fgf signaling during zebrafish somitogenesis

Hung-Chieh Lee [a], Wei-An Tseng [a], Fang-Yi Lo [a], Tzu-Ming Liu [b], Huai-Jen Tsai [a,*]

[a] Institute of Molecular and Cellular Biology, National Taiwan University, Room 307, Fisheries Science Building, No. 1, Section 4, Roosevelt Road, Taipei, Taiwan
[b] Institute of Biomedical Engineering, National Taiwan University, Taiwan

ARTICLE INFO

Article history:
Received for publication 22 April 2009
Revised 11 September 2009
Accepted 1 October 2009
Available online 8 October 2009

Keywords:
FoxD5
Fgf
Somitogenesis
Zebrafish

ABSTRACT

The transcription factor *FoxD5* is expressed in the paraxial mesoderm of zebrafish. However, the roles of *FoxD5* in anterior pre-somitic mesoderm (PSM) during somitogenesis are unknown. We knocked down *FoxD5* in embryos, which resulted in defects of the newly formed somites, including loss of the striped patterns of anterior–posterior polarity genes *deltaC*, *notch2*, *notch3* and *EphB2a*, as well as the absence of *mespa* expression in S-I. Also, the expression of *mespb* exhibited a 'salt and pepper' pattern, indicating that *FoxD5* is necessary for somite patterning in anterior PSM. Embryos were treated with SU5402, an Fgf receptor (FGFR) inhibitor, resulting in reduction of *FoxD5* expression. This finding was consistent with results obtained from *Tg(hsp70l:dnfgfr1-EGFP)pd1* embryos, whose dominant-negative form of FGFR1 was produced by heat-induction. Loss of *FoxD5* expression was observed in the embryos injected with *fgf3*-/*fgf8*-double-morpholinos (MOs). Excessive *FoxD5* mRNA could rescue the defective expression levels of *mespa* and *mespb* in *fgf3*-/*fgf8*-double morphants, suggesting that Fgf signaling acts as an upstream modulator of *FoxD5* during somitogenesis. We concluded that *FoxD5* is required for maintaining anterior–posterior polarity within a somite and that the striped pattern of *FoxD5* in anterior PSM is mainly regulated by Fgf. An Fgf-FoxD5-Mesps signaling network is therefore proposed.

Introduction

Somite formation is defined as the reiterated subdivision of paraxial mesoderm into paired, epithelial spheres of cells on either side of the midline, and it is a common occurrence in many species. Studies reveal that there is a pre-patterning process in the anterior of the pre-somitic mesoderm (PSM) before the morphological appearance of somite pairs. Cooke and Zeeman (1976) proposed a clock and wavefront model to explain the pattern formation of PSM. They explain that a clock mechanism controls the cell oscillations between anterior and posterior somitic identities in the PSM. During this process, the position of future somite boundaries is selected in the PSM. Both anterior and posterior somitic identities are responsible for boundary formation. In fact, roles in somitogenesis have been postulated for a variety of transcription factors and signaling modulators, such as Fibroblast growth factor (Fgf), bone morphogenetic protein (BMP), T-box gene, Hedgehog (Hh), and Wnt (Nikaido et al., 2002; Kimelman 2006; Ozbudak and Pourquié, 2008). Besides these signaling modulators, some basic basic helix-loop-helix (bHLH) genes also play important roles in somite patterning, such as Notch signaling, which involves the *mesp* and *hes*/*her* genes (Takke and Campos-Ortega 1999; Takahashi et al. 2000).

The winged-helix or Forkhead box (Fox) proteins comprise a highly conserved family of transcription factors, which all share the highly conserved 'forkhead' DNA-binding domain (Kaestner et al., 2000). Based on conserved residues at distinct positions in the DNA binding domain, more than 10 different classes of *Fox* genes have been described. Similar to other transcription factor families, *Fox* genes are involved in many different developmental processes, such as mesoderm patterning during early embryogenesis. More than 100 *Fox* genes have been identified across species from yeasts to humans (Wijchers et al., 2006). In mice, loss of *Foxa2* leads to lack of notochord and other midline structures (Weinstein et al., 1994). *Foxf1* is required for lateral plate mesoderm and extra-embryonic mesoderm tissue development (Kalinichenko et al., 2001). *Fox* genes also play important roles during somitogenesis. *Foxc1* and *Foxc2* are necessary for paraxial mesodermal fate induction (Wilm et al., 2004). *Foxb1*- and *Foxk1*-deficient mice display defects in the muscle (Garry et al., 2000). In zebrafish, Odenthal and Nüsslein-Volhard (1998) classified zebrafish *Fox* genes and showed that the Class V *Fox* genes are all expressed in the somite and paraxial mesoderm, including *FoxD1, FoxD3* and *FoxD5*. Mouse *FoxD1* mutant displayed normal morphology, suggesting that *FoxD1* may not be a key factor during somitogenesis (Hatini et al., 1996). Meanwhile, although it is well known that zebrafish *FoxD3* mediates *myf5* expression during early somitogenesis (Lee et al., 2006), the roles of *FoxD5* during somitogenesis have never been reported in any species. Thus, in this report, we

* Corresponding author. Fax: +886 2 2363 8483.
E-mail address: hjtsai@ntu.edu.tw (H.-J. Tsai).

0012-1606/$ – see front matter © 2009 Elsevier Inc. All rights reserved.
doi:10.1016/j.ydbio.2009.10.001

focus on the roles of zebrafish *FoxD5* during somitogenesis. We found that loss of *FoxD5* results in a disordered morphogenesis of somites, suggesting that *FoxD5* is necessary for somite polarity. While we found that *FoxD5* is regulated by both Fgf and Hh signaling, Fgf signaling appears to be the major pathway.

Materials and methods

Zebrafish husbandry and microscopy

Zebrafish were raised as described in Westerfield (1995). Mutant alleles, *lia/fgf3* ^{t21142} (Herzog et al., 2004) and *ace/fgf8*^{ti282a} (Roehl and Nüsslein-Volhard, 2001), and transgenic line *Tg(hsp70l:dnfgfr1-EGFP)pd1*, which provides the overexpression of dominant-negative FGFR1 under the control of the heat-shock-cognate-70-kd protein (hsp70) promoter (Lee et al., 2005), were used in this study. Fluorescence was visualized with a fluorescent stereomicroscope (MZ FLIII, Leica) and a confocal spectral microscope (TCS SP5, Leica). The harmonics optical microscopy (HOM), which including the higher second and third harmonic generations of laser-induced fluorescence, was used to examine the structures of tissues and organs in live zebrafish embryos as it was described previously (Sun et al., 2004).

Whole-mount in situ hybridization (WISH) and immunohistochemical detection

The coding sequence of *FoxD5* was isolated by RT-PCR, inserted into plasmid pGEMTeasy (Promega) and confirmed by sequencing. Riboprobes for detection of the following cDNAs were used: *cb1045, deltaC, deltaD, FoxC1a, her1, her1* intron (Kawamura et al., 2005b), *myf5, myod, myogenin, mespa, mespb, tbx24, notch2, notch3, paraxis,* (Sawada et al., 2000), *papc* (Yamamoto et al., 1998) and *ripply1* (Kawamura et al., 2005a). WISH and immunohistochemical detection were described previously (Lee et al., 2006), except that the hybridization method of the *her1* intron probe was carried out as described by Gajewski et al. (2003). The mouse S58 anti-slow myosin antibody (Developmental Studies Hybridoma Bank) was used at a dilution of 1:10 on embryos fixed in Carnoy's fixative and was visualized with a 1:16 dilution of donkey anti-mouse IgG-TR antibody (Santa Cruz Biotechnology). The mouse MF20 anti-myosin heavy chain antibody (Developmental Studies Hybridoma Bank) was used at a dilution of 1:10 on PFA-fixed embryos and was visualized with a 1:16 dilution of goat anti-mouse IgG-FITC antibody (Santa Cruz Biotechnology).

Injection experiments

The antisense morpholino oligonucleotides (MO) specific for silencing the translation of mRNA for *FoxD5, tbx24, fgf3, fgf8, mespa, mespb* and *p53* were designed to block either the translation start site or 5′-untranslated region (Gene Tools, LLC). *FoxD5*-MO1 (5′-GTTCGTAATCCTGCGAGAGGGTCAT-3′), *FoxD5*-MO2 (5′-GTTGGAGACCCTAAATGTGCTGGAC-3′), *tbx24*-MO (5′-CATTTCCA-CACCCAGCATGTCTCGG-3′) (Kawamura et al., 2005a), *fgf8*-MO (5′-GAGTCTCATGTTTATAGCCTCAGTA-3′) (Raible and Brand, 2001), *fgf3*-MO (5′-CATTGTGGCATGGCGGGATGTCGGC-3′) (Phillips et al., 2001), *mespa*-MO (5′-GAAGAGAAAACGTGGAGGCGTCCAT-3′) (Hart et al., 2007), *mespb*-MO (5′-TCGGTTCTTGCTTGAGGTTTGCATG-3′) (Kawamura et al., 2005a) and *p53*-MO (5′-GCGCCATTGCTTTGCAAGAATTG-3′) were used. The corresponding control MOs for *FoxD5*-, *mespa*- and *mespb*-MO were *FoxD5*-5mis-MO (5′-GTTgGTAATgCTcCGAGAcGGT-gAT-3′), *mespa*-5mis-MO (5′-GAAcAcAAAACcTGGAGcCGTCgAT-3′), and *mespb*-5mis-MO (5′-TCcGTTgTTcCTTGAGcTTTGgATG-3′), respectively. The mismatched nucleotides to the experimental MOs are indicated by lower case. Microinjection was performed using published procedures (Westerfield, 2000).

To avoid *FoxD5*-MO1 binding to the synthesized *FoxD5* mRNA that we microinjected for the rescue experiment, a truncated form of zebrafish *FoxD5* (*tFoxD5*) mRNA, which lacks the sequence complementary to *FoxD5*-MO1, was generated by PCR and cloned into pCS2+. The mRNAs for eGFP, full-length-*FoxD5* and truncated-*FoxD5* were generated with the SP6 Message Machine Kit (Ambion).

Drug treatment

The drugs SU5402 and cyclopamine are widely used inhibitors of Fgf receptor (FGFR) activation (Mohammadi et al., 1997) and Hh activation (Cooper et al., 1998), respectively. SU5402 (CalBiochem) was dissolved in dimethylsulfoxide (DMSO), and cyclopamine was dissolved in 95% ethanol. Embryos were immersed with either 30 μM SU5402 or 100 μM cyclopamine from the 60% epiboly-stage to bud-stage. Treatment was performed in a 3-cm Petri dish filled with 30 embryos in a total volume of 2 ml embryo medium. No effect was observed by exposing embryos to either DMSO or ethanol alone at the same concentration used for the experimental treatments. For each experiment, a portion of the embryos was collected and fixed at 12 h in 4% paraformaldehyde/PBS for WISH.

Results

Expression of the zebrafish FoxD5 gene during embryonic development

When we studied the spatiotemporal expression of *FoxD5* during zebrafish embryogenesis by RT-PCR, we found that *FoxD5* mRNA was maternally inherited (Fig. 1A). WISH showed that transcripts of *FoxD5* were detected through the embryos, especially in the dorsal organizer during gastrulation (6 h post-fertilization (hpf); Fig. 1B). As gastrulation proceeded, a strong expression was observed at the adaxial cells flanking the future notochord, tailbud, lateral plate mesoderm (Fig. 1C) and head region (data not shown). During bud-stages, *FoxD5* transcripts extended into the future head (data not shown), two stripes in the adaxial cells, two stripes in the paraxial mesoderm, and tailbud (Fig. 1D). During 12–24 hpf, *FoxD5* transcripts were detected in the head region, the adaxial cells, anterior PSM and tailbud (Figs. 1E–H). During 24–36 hpf, *FoxD5* transcripts were still strongly exhibited in the head region, but they were gradually reduced at the tail region (data not shown).

To determine whether the stripe expressions of *FoxD5* are in the newly formed somites or in the anterior PSM, we compared the expression of *FoxD5* with other genes reported to be expressed in this specific region and found that dynamic stripe expression of *FoxD5* was in both the anterior PSM and newly formed somites (Figs. 1I, J). Furthermore, double ISH with *FoxD5* and *mespa* probes revealed that *FoxD5* was expressed in the S-I and S-II at 12 hpf (Fig. 1K) and co-localized with *mespa* transcripts. Meanwhile, double ISH with *FoxD5* and *her1* probes showed that *FoxD5* mRNA was only expressed in the S-I at 14 hpf, and the expression domains of *FoxD5* and *her1* were separated and juxtaposed against each other (Fig. 1L).

Knockdown of FoxD5 affected the somite boundary formation and led to a segmentation defect

Because *FoxD5* mRNA was expressed in the anterior PSM and adaxial cells, we proposed that *FoxD5* might play a role in somite formation and differentiation. To study whether *FoxD5* is required for somitic segmentation, we specifically blocked the translation of *FoxD5* mRNA using two MOs, *FoxD5*-MO1 against the sequence overlapping the translation start site and *FoxD5*-MO2 against the 5′-untranslated sequences. The same phenotypes were observed when these two MOs were microinjected, confirming the specific defects of embryos induced by injection of MOs (Supplementary Table S1). When 1–4 ng of *FoxD5*-MO1 was microinjected, the morphants displayed

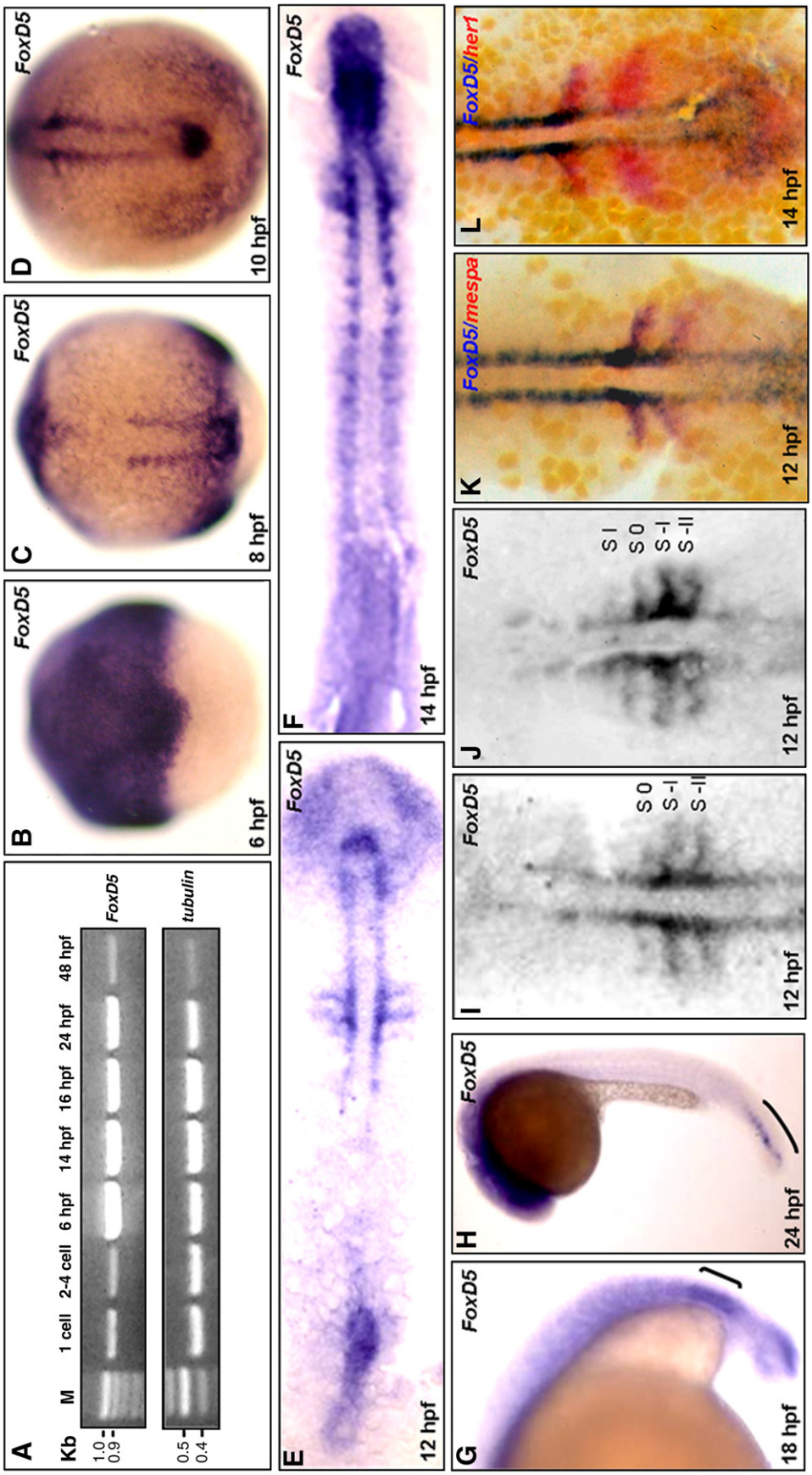

Fig. 1. The spatiotemporal expression of *FoxD5* during zebrafish embryogenesis. Using RT-PCR to detect the transcripts of *FoxD5* during the developmental stages as indicated. Lane M was a marker, and *tubulin* was an internal control (A). Using WISH to reveal that *FoxD5* was expressed ubiquitously at 6 hpf (B), expressed in the yolk synthetic layer and adaxial cells at 8-hpf (C), and expressed in the anterior PSM, adaxial cells and tailbud at 10- (D) 12- (E) and 14-hpf (F). During 18–24 hpf, *FoxD5* in the adaxial cells was down-regulated gradually (black blanket), but it was still expressed in the head and tailbud (G, H). During 12 hpf, dynamic stripe expressions of *FoxD5* in the anterior PSM (S0-S-II) and newly formed somites (SI) were observed (I, J). Double ISH of *mespa*, *her1* (labeled in red) and *FoxD5* (labeled in blue) expressions during 12 and 14 hpf showed that *FoxD5* was expressed in the anterior PSM from S-I to S-II (K, L).

defects in the head and trunk at 24 hpf (Figs. 2B, C). Most abnormalities were mild, including slightly reduced head size and disordered somite with an irregular boundary (Figs. 2C, F), but other abnormalities were more severe, including greatly reduced head size and distorted axis (Figs. 2B, E). Although *FoxD5* morphants did not lose their somite boundaries, the arrays of paired somites became irregular (Fig. 2D vs. E, F). Moreover, the expression of somite border marker *cb1045* was lost in the *FoxD5* morphants (Figs. 2G, H), suggesting that *FoxD5* is necessary for somite formation.

To verify the defective specificity induced by *FoxD5*-MO1, we co-injected with *FoxD5*-MO1 and a truncated form of *tFoxD5* mRNA, in which the first seven amino acids of the N-terminus of FoxD5 were deleted. Under these conditions, *FoxD5*-MO1 specifically blocked the endogenous *FoxD5* mRNA, but it failed to block the *tFoxD5* mRNA we

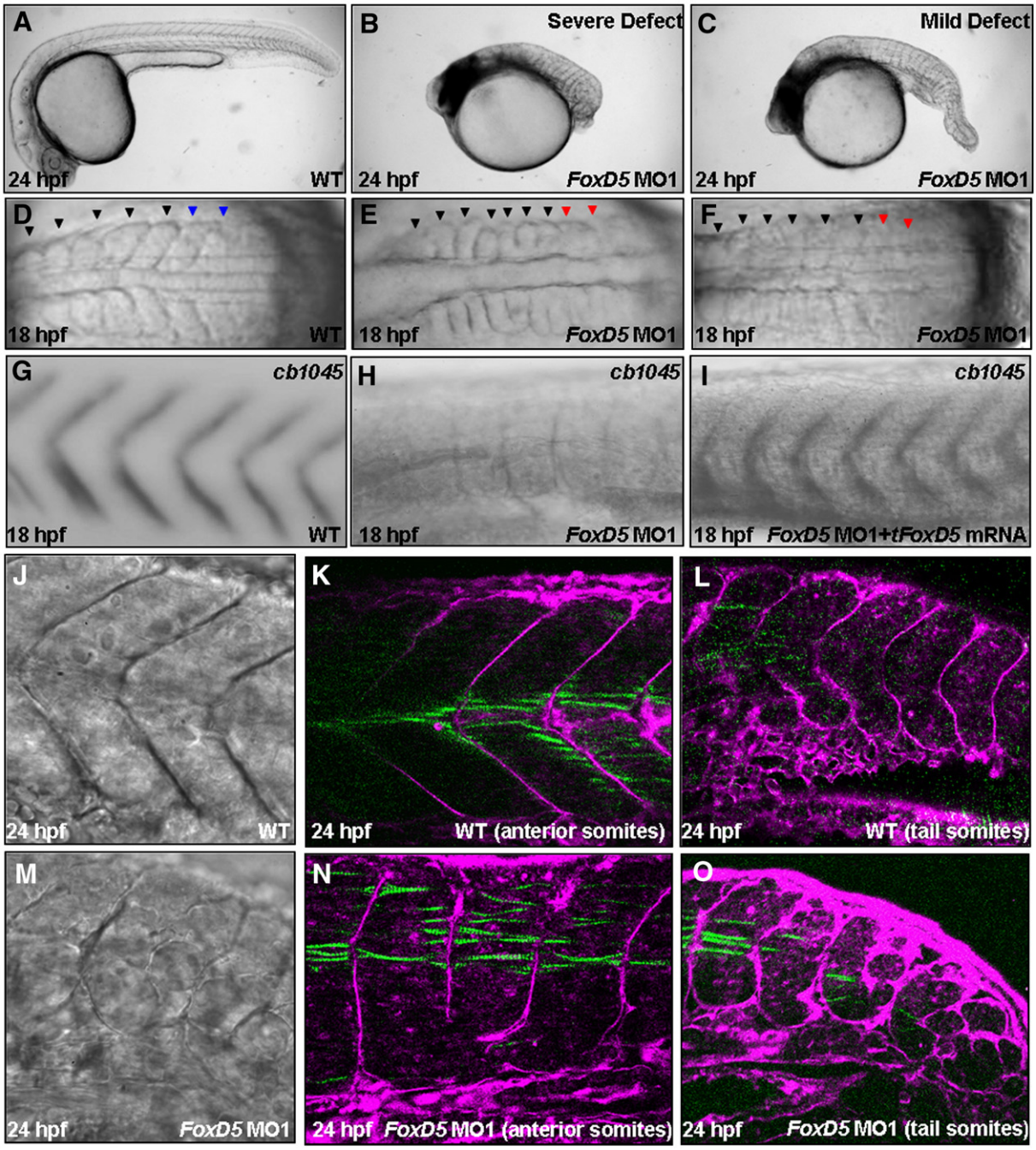

Fig. 2. Loss of FoxD5 function resulted in loss of somite polarity during somitogenesis. The *FoxD5*-MO1-injected embryos with abnormal phenotypes were categorized as having severe defects, such as smaller head size and distortion axis (B), and mild defects, such as reduced head and disordered somites with irregular boundary (C). Dorsal views of trunk somites in WT embryos (WT; D) and *FoxD5*-MO1-injected embryos (E, F) at 18 hpf. In WT embryos, column-shaped, maturely formed somites (indicated by black arrowheads) and two newly forming somites S-I and S-II (blue arrowheads) were observed. Meanwhile, in *FoxD5* morphants, wider and more raggedly formed mature somites (black arrowheads) and newly forming somites, but with irregular somitic furrows (red arrowhead), were observed. The expressions of *cb1045* at 18-hpf in WT embryos and *FoxD5* morphants were also studied. The *cb1045* was specifically observed in the somite borders of WT embryos (G), but it was lost in *FoxD5* morphants (H). Co-injection of *FoxD5*-MO1 and *tFoxD5* mRNA enabled embryos to rescue the defective expression of *cb1045* induced by *FoxD5*-MO1 alone (I). *In vivo* HOM sectioning of WT embryos (J–L) and *FoxD5* morphants (M–O) at 24 hpf was examined under bright field (J, M) and dark field microscopes (K, L, N, O). The morphological structures, including skin and somite boundaries, which are labeled in purple, were observed by third harmonic generation signal, whereas muscle fibers, which are labeled in green, were observed by second harmonic generation emissions. Compared to the WT embryos (K, L), the structure of the somites in the *FoxD5* morphants was disordered (N, O).

microinjected. We noticed that the *tFoxD5* mRNA should be as functional as the full-length of *FoxD5* mRNA because no significant difference of defects was observed between embryos injected with the *tFoxD5* mRNA and *FoxD5* mRNA (Supplementary Table S2). In the rescue experiment, the defective phenotype caused by *FoxD5*-MO1 was not rescued by co-injection of *egfp* mRNA with *FoxD5*-MO1 (Supplementary Table S1). However, embryos displaying the normal phenotype dramatically increased when the *tFoxD5* mRNA was co-injected with *FoxD5*-MO1 (Supplementary Table S1, Figs. S1D, D'). When we microinjected 4–8 ng of control *FoxD5*-5mis-MO, which contains five mismatched nucleotides against *FoxD5*-MO1, no phenotype was observed (Supplementary Table S1; Figs. S1E, E'). Similarly, the number of embryos displaying the normal phenotype dramatically increased when full-length *FoxD5* mRNA was co-injected with *FoxD5*-MO2 (Supplementary Table S1). Moreover, the excessive *tFoxD5* mRNA enabled embryos to rescue the disordered somite boundary caused by *FoxD5*-MO1, and these embryos were able to regain *cb1045* expression (Fig. 2I). Besides, to rule out the possibility that the defects in *FoxD5* morphants were caused by the toxicity of MOs, we co-injected 3 ng of *FoxD5*-MO1 and 6 ng of *p53*-MO. Results showed that the somitic boundaries were not rescued, but instead were still disorganized (Fig. S1C'), indicating that the structural defects in somite and the reduction of *cb1045* expression (Fig. 2H vs. I) in *FoxD5*-MO1-injected embryos were specific and dependent upon *FoxD5* loss of function.

To understand which kind of somite defects occurred in the *FoxD5* morphants, we used *in vivo* sectioning to analyze the somite development of wild-type (WT) embryos and *FoxD5* morphants by HOM and laser-induced fluorescence higher harmonic generations. The epidermis, somite boundary and notochord were clearly identified by third harmonic generation signals (purple labels in Figs. 2K, L, N, O). The myotomes, which are composed of collaterally organized myosin and actin filaments, appeared strongly by second harmonic generation emissions as a result of their highly organized nano-structures (green labels in Figs. 2K, L, N, O). The trunk and tail somites of WT embryos at 24 hpf were exhibited distinctly (Figs. 2K, L). However, the trunk somite in the *FoxD5* morphants showed incomplete development (Figs. 2M, N), while the tail somite displayed a severely disordered structure. Abnormally disorganized structures were observed in the tail somites (Fig. 2O), indicating that the development of somites is impeded in *FoxD5* morphants. In addition, the abnormal morphology of somite structure in *FoxD5* morphants suggested that the segmental patterning is disturbed as well. Thus, we proposed that the stripe expression of *FoxD5* in the anterior PSM is required for normal formation of somite in furrow.

The establishment of segmental pre-pattern was processed normally in the FoxD5-knockdown embryos

Before epithelial somites are formed, precise anterior and posterior domains are established in the somite primordial. It has been reported that Notch-dependent signaling is required during this step (Johnson et al. 2000; Sawada et al. 2000; Ozbudak and Pourquié, 2008). The oscillatory behavior in the PSM is manifested in the zebrafish embryo by periodic waves of expressions of *deltaC* and *her1* that appear to extend anteriorly from the tail bud (Jiang et al. 2000; Goldbeter and Pourquié, 2008; Holley et al., 2000). In this study, we found that the expression patterns of *deltaC* and *her1* in the PSM of *FoxD5*-MO1-injected embryos were presented as a dynamic scheme of periodically changing broad and narrow strips, which were similar to those in the PSM of WT embryos (Figs. 3A, C vs. B, D). Similar to the WT embryos, the dynamic expression of *her1* in the PSM of the *FoxD5*-MO1-injected embryos was also normal (Fig. 3B vs. F). In addition, the cyclical expression of the *her1* intron probe was also detected in the WT embryos and the *FoxD5* morphants (data not shown). Thus, knockdown of the *FoxD5* gene in zebrafish embryos did not affect gene oscillation in the posterior PSM. However, unlike the *deltaC* expression in the somite of WT embryos, the striped expression of *deltaC* was not sustained in the somites of *FoxD5*-MO1-injected embryos during 10–14 hpf (Figs. 3B, D). These evidences indicate that the first step of segmentation such as the establishment of segmental pre-pattern is not affected by *FoxD5* inhibition, but rather, that synchronized oscillatory behavior does occur in the PSM of *FoxD5*-MO1-injected embryos. Thus, the disorganized structure of somites in *FoxD5* morphants might be because *FoxD5* expression is absent in the anterior PSM, not because *FoxD5* is absent in tailbud and posterior PSM.

The anterior–posterior polarity in somites was lost in the FoxD5 morphants

The reduced *deltaC* expression in the somites of *FoxD5* morphants suggested that the anterior–posterior polarity in the somites might be affected. We examined the expressions of *notch3* and *notch2*, which label anterior and posterior somites, respectively. We found that expressions of *notch2* (Fig. 3G) and *notch3* (Fig. 3I) appeared in striped pattern in the somites of WT embryos. However, instead of a striped pattern presented in the somites of WT, a smeared signal was observed in this same region of the *FoxD5*-MO1-injected embryos (Figs. 3H, J). These results suggest that *foxD5* is necessary for normal somitogenesis and that *FoxD5* functions in controlling the anterior–posterior polarity of somites.

Since the ectopic expression of Eph/Ephrin signaling leads to abnormal somitogenesis (Durbin et al. 1998), we examined the expression of *ephrinB2a* in *FoxD5* morphants. Results showed that the striped pattern of *ephrinB2a* was lost, and a smeared pattern throughout the somitic region in *FoxD5* morphants was observed (Fig. 3K vs. L). Mice lacking *paraxis* do not form somite epithelium and show severe defects of muscle (Burgess et al., 1995; 1996). Here, however, it is the striped pattern of *paraxis* that was lost in the somites of *FoxD5*-knockdown embryos (Fig. 3M vs. N). The paraxial protocadherin, *papc,* a member of the cadherin superfamily, is an important regulator during somitogenesis (Yamamoto et al., 1998). Interestingly, while *papc* expression domains located at S-I and S-II were still present in MO-injected embryos (Fig. 3O), the stripes of *papc* mRNA were ectopically expressed in the formed somites (Fig. 3P). We also found that *papc* transcripts were increased greatly in the *FoxD5* morphants during bud-stage (Supplementary Fig. S2), suggesting that *FoxD5* might play a role in inhibiting *papc* expression in the anterior PSM when somites start to form. Taken together, the defective expressions of the genes we studied in the somites of *FoxD5* morphants indicated that *FoxD5* is an essential factor for anterior–posterior patterning during somite furrow formation.

The anterior/posterior identity of cells in the anterior PSM was impeded in FoxD5-MO1-injected embryos

Next, we focused on the anterior PSM where *FoxD5* is expressed in striped pattern. The *mesp* genes play a conserved role during segmental patterning of the mesoderm in vertebrate embryos by specifying segmental boundaries and anterior–posterior segmental polarity (Sawada et al., 2000). Previous studies (Takahashi et al., 2000) revealed that *mesp* genes specifically affect Notch signaling in the anterior PSM. In this study, we found that both *mespa* and *mespb* genes were expressed in overlapping domains in the anterior of the somite primordia S-I and S-II during somitogenesis in zebrafish embryos (Figs. 4A, C), as Durbin et al. (2000) and Sawada et al. (2000) reported. In addition, a transient band of *mespb* expression was observed in the forming somite S0 (Fig. 4C). However, we observed that the expression of *mespa* in S-I was lost in the *FoxD5*-MO1-injected embryos (Fig. 4B). In contrast, while *mespb* expression lost its

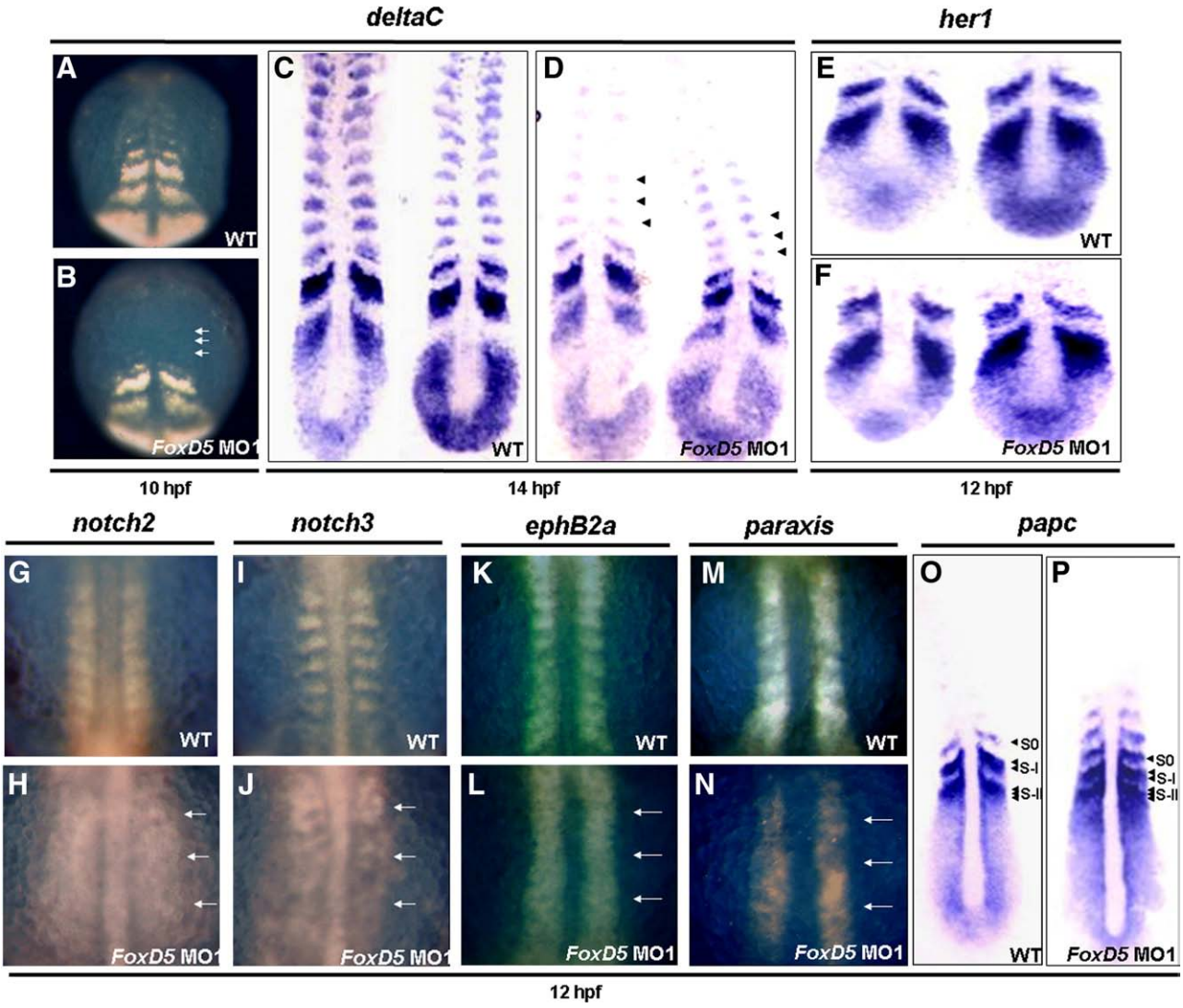

Fig. 3. Loss of FoxD5 function did not affect the wavefront and clock in the PSM, but did cause defects in the somites and anterior PSM where the somites were formed. By WISH, the expressions of *deltaC*, *her1*, *notch2*, *notch3*, *ephB2a*, *paraxis* and *tbx24*, as well as *FoxD5* in wild-type embryos (WT), *FoxD5* morphants (*FoxD5* MO) and *tbx24* morphants (*tbx24* MO), were observed at 10–14 hpf as indicated. Compared to WT embryos (A, C), *FoxD5* morphants showed normal variation in the pattern of *deltaC* expression, but the striped expression was not maintained in the region where the somites (arrowhead) should have been presented (B, D). The expression of *her1* showed a normal oscillation in WT (E) and *FoxD5* morphants (F). The striped patterns of *notch2, notch3, ephB2a* and *paraxis* in the somites were normal in WT embryos (G, I, K, M), but they were disordered in *FoxD5* morphants (H, J, L, N). Expression of *papc* appeared strongly at somites from S-II to S0. Although the intensity was decreased from posterior to anterior in WT embryos (O), the expression of *papc* was ectopically increased and showed 5–6 strong signal bands in *FoxD5* morphants (P).

striped pattern, it appeared as a "salt and pepper" pattern in the *FoxD5*-deficient embryos (Fig. 4D). Therefore, even though *FoxD5* affects *mespa* and *mespb* differentially, it is still required for normal expression of these two genes in the anterior PSM.

FoxD5 did not function in the segmental pre-pattern

Zebrafish T-box transcription factor Tbx24 is necessary for somite formation (van Eeden et al., 1996; Nikaido et al., 2002). In WT embryos, *tbx24* was expressed in the PSM and in the anterior part of forming somites S0 to SII (Fig. 4E). Although *tbx24* expression in the PSM of *FoxD5* morphants was as same as that of WT embryos, *tbx24* failed to maintain segmented expression in somites when *FoxD5* was absent (Fig. 4F). In other words, *FoxD5* was still expressed in the tailbud and adaxial cells in the *tbx24* morphants, but not in the anterior PSM, specifically, S0 to S-II (Fig. 4G vs. H). Therefore, we suggested that *FoxD5* might be downstream of *tbx24* and that, therefore, *FoxD5* plays a role in the anterior PSM to maintain somitic anterior–posterior polarity, but not segmental pre-pattern.

The modulation of Fgf and Hh signaling on FoxD5 expression

Next, we attempted to study which signaling is necessary for *FoxD5* expression during somite formation in zebrafish embryos. The Fgf signaling pathway in the PSM controls cell maturation and the positioning of segmental boundary (Sawada et al., 2001; Dubrulle and Pourquié, 2004; Wahl et al., 2007). To investigate the temporal requirement for Fgf signaling, we immersed embryos in embryo medium containing SU5402, an FGFR inhibitor. The SU5402-treated embryos were incubated, starting at 60% epiboly, until 6–8 somite-stages. To demonstrate the effectiveness of the treatment, a subset of the embryos was fixed immediately and processed for WISH of *FoxD5*. In all SU5402-treated embryos, the *FoxD5* transcripts were barely detectable in the anterior PSM (Fig. 5B); however, we could still observe the somite structure (data not shown), although the *myod* signals were greatly reduced (Fig. 5I). Moreover, embryos derived from outcrossing a homozygous strain of *Tg*(*hsp70l:dnfgfr1-EGFP*)*pd1* fish were treated with heat shock induction at 37 °C for 1 h at 8–9 hpf, with analysis of the *FoxD5* transcripts during 12 hpf. Although we

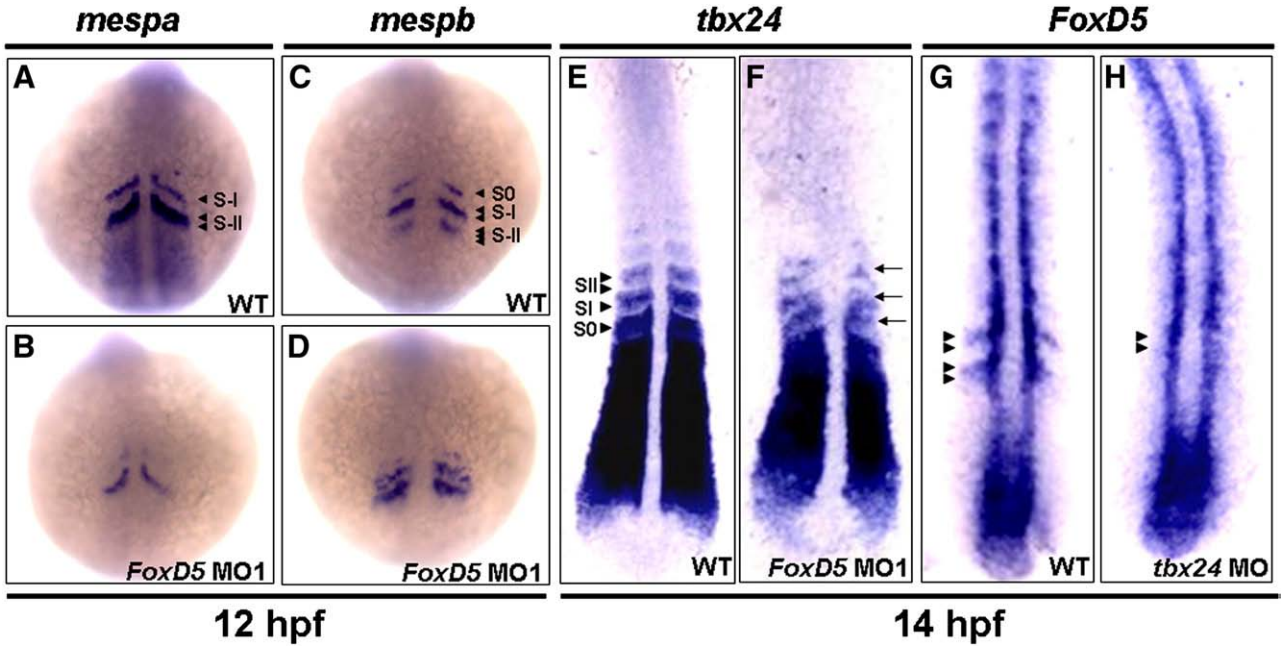

Fig. 4. Effect of inhibiting FoxD5 protein synthesis on the expression of *mespa* and *mespb*. By WISH, the expressions of *mespa*, *mespb* and *papc* in wild-type embryos (WT) and *FoxD5* morphants (*FoxD5* MO) were observed at 12–24 hpf as indicated. *mespa* was expressed at somites S-I and S-II in WT (A), but was greatly reduced in *FoxD5* morphants (B). *mespb* was detected from S0 to S-II as a striped pattern in WT (C), but failed to maintain a striped expression (D). Expression of *tbx24* was detected in the PSM and the anterior part of formed somites from S0 to SII in WT (arrowheads in E). Although *tbx24* expression was unchanged in the PSM, it failed to maintain a segmented expression at the somite region in the *FoxD5* morphants (arrows in F). *FoxD5* was expressed at tailbud, adaxial cells, and forming somites in WT (arrowheads in G), whereas *FoxD5* was still expressed at tailbud and adaxial cells, but was not at the forming somite region in the *tbx24* morphants (H).

observed somite formation in these heat shock-treated embryos, WISH of the *FoxD5* transcripts revealed that inhibition of Fgf signaling greatly reduced *FoxD5* expression (Fig. 5C). When embryos were treated with SU5402 for 4 h, starting at 12 hpf, with analysis of the *FoxD5* transcripts during 16 hpf, we found that *FoxD5* expression was still greatly reduced (data not shown). Additionally, when embryos derived from *Tg*(*hsp70l:dnfgfr1-EGFP*)*pd1* were treated with heat shock induction at 10–11 hpf, with analysis of the *FoxD5* transcripts during 12 hpf, we observed that these embryos continued to display a reduction of *FoxD5* transcripts (data not shown). These findings strongly suggested that the striped expression of *FoxD5* in the anterior PSM is dependent on Fgf activity. We also noticed that the *fgf8* and *fgf3* mutants showed slightly reduced expressions of *FoxD5* in the adaxial cells and anterior PSM (Figs. 5D, E). However, *fgf3*-/*fgf8*-double morphants showed that the expression of *FoxD5* was almost lost in the adaxial cells and the anterior PSM at 12 hpf (Fig. 5F), suggesting that Fgf3 and Fgf8 might have redundant function in regulating *FoxD5* expression. Taken together, we proposed that Fgf signaling is an upstream modulator of *FoxD5* during somitogenesis.

Hh signaling has been shown to promote myogenesis in both fish and amniotes (Ingham and McMahon, 2001; Borello et al., 2006). After we treated embryos with the Hh inhibitor cyclopamine, starting at 60% epiboly, 80% epiboly or bud-stages, and ending at 6–8 somite-stages, we performed WISH which showed that *FoxD5* was detected in the somites and anterior PSM, but was lost in the adaxial cells in cyclopamine-treated embryos (Fig. 6A vs. F). A slightly enhanced and extended expression of *FoxD5* in the anterior PSM was observed in cyclopamine-treated embryos (Fig. 6A vs. F), suggesting that Hh signaling is necessary to inhibit *FoxD5* expression in the anterior PSM. In addition, the ectopic expression of *FoxD5* did not cause the ectopic expressions of *mespa* and *mespb* (Figs. 6C, D vs. H, I). These results suggest that some other type of signaling represses the expression of *mesps*, such as *ripply1,* and may still be present in the somites of cyclopamine-treated embryos (Fig. 6E vs. J). On the other hand, *myod* transcripts were only detected in the somites, but not in the adaxial cells (Fig. 6B vs. G). Thus, the loss of FoxD5 and Myod in the adaxial cells of cyclopamine-treated embryos was the result of incomplete development of the adaxial cell structure. Therefore, we concluded that Hh activity is required for inhibition, rather than induction, of *FoxD5* expression.

Excessive FoxD5 mRNA could rescue the defective expression levels, but not the striped patterns, of mespa and mespb in the absence of Fgf signaling

We have demonstrated that *FoxD5* plays roles in modulating *mespa* and *mespb* expressions and that *FoxD5* is regulated by Fgf signaling. However, precisely which factor or signaling is required for the expression of *mesps* during somitogenesis is unclear. To define further the molecular network among Fgf, FoxD5 and Mesps during zebrafish somitogenesis, we analyzed the expressions of *mespa* and *mespb* in the *fgf3* mutant, the *fgf8* mutant and the *fgf3*-/*fgf8*-double-MO-injected embryos. Results showed that two stripes of *mespa* expression in the anterior PSM were slightly reduced in both *fgf3* and *fgf8* mutants (Fig. 7A vs. C, E), while *mespa* was greatly reduced in the *fgf3*-/*fgf8*-double morphants (Fig. 7I). Interestingly, the pattern of *mespa* expression in the *fgf8* mutant was similar to that which appeared in the *FoxD5*-MO1 morphants (Fig. 4B vs. Fig. 8A). That is, two or three stripes of *mespb* in the anterior PSM were slightly reduced in both the *fgf3* and *fgf8* mutants (Fig. 7B vs. D, F), but greatly reduced in the *fgf3*-/*fgf8*-double morphants (Fig. 7J). In embryos derived from the transgenic line *Tg*(*hsp70l:dnfgfr1-EGFP*)*pd1* and treated with heat-shock induction at 10–11 hpf, it was found that both *mespa* and *mespb* at 12 hpf were greatly reduced (Figs. 7G, H). Furthermore, when *FoxD5* mRNA was co-injected with *fgf3*-/*fgf8*-double-MOs, the expression levels of *mespa* and *mespb* were nicely rescued (Figs. 7I, J vs. K, M). However, we noticed that the stripe patterns of *mespa* and *mespb* were not restored by injection of *FoxD5* mRNA in the *fgf3*-/*fgf8*-double morphants. Thus, we hypothesized that some factor, other than *FoxD5*, might be the target of Fgf signaling in regulating the striped expression of *mesps*.

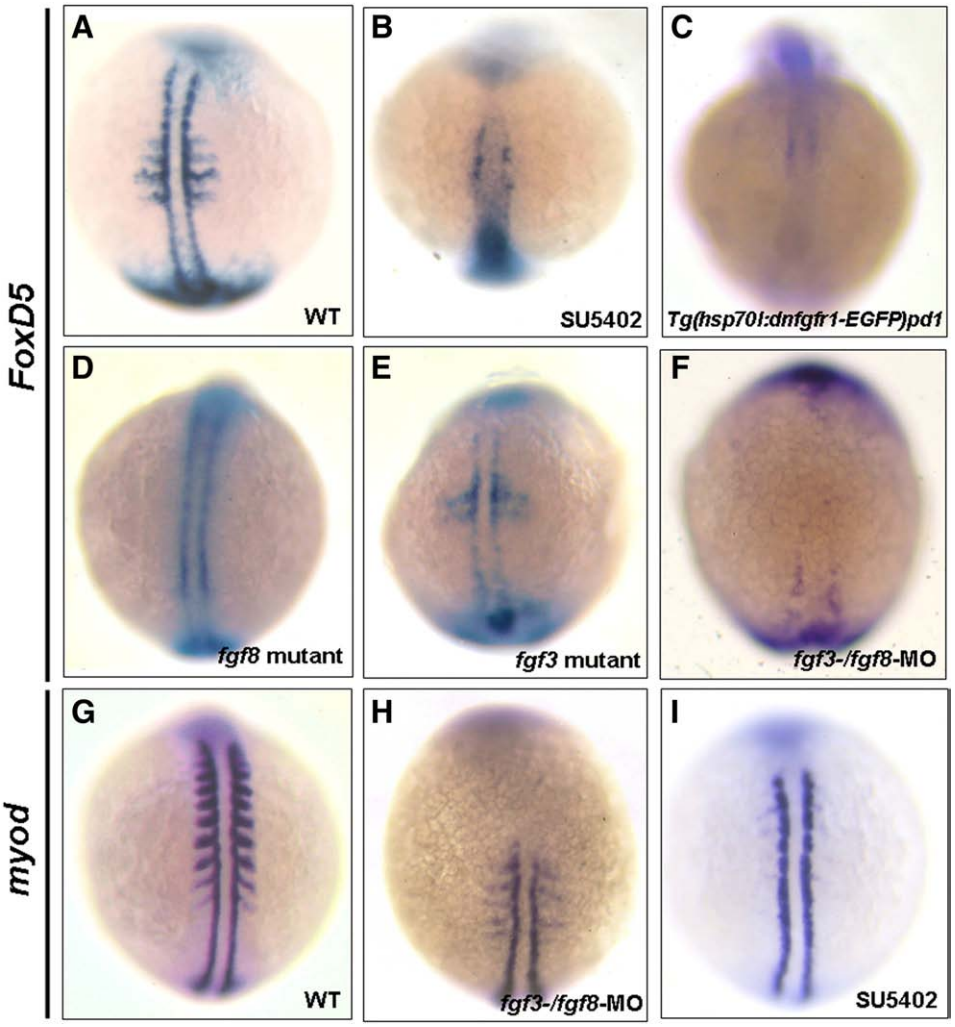

Fig. 5. Fgf signaling was necessary for *FoxD5* expression during early somitogenesis. Using WISH to detect the expression of *FoxD5* and *myod* in wild-type (WT) embryos, *fgf3* mutants, *fgf8* mutants, and embryos treated with different materials, as indicated. Embryos were incubated for 6 h in SU5402, starting at 6 hpf; heterozygous strain of fish derived from transgenic line *Tg(hsp70l:dnfgfr1-EGFP)pd1* were crossed with WT individuals, and their progeny were heat shocked at 10 hpf for 1 h, followed by WISH analysis at 12 hpf. In both sets of experiments, the expression of *FoxD5* in the anterior PSM and adaxial cells was greatly reduced (B, C). In *fgf8* (D) and *fgf3* mutants (E), the expression of *FoxD5* was slightly reduced. However, in *fgf3*-/*fgf8*-double-MO-injected embryos, *FoxD5* transcripts were almost lost (F). In WT, *myod* was detected in the somites and adaxial cells (G). While *myod* could still be detected in the somites and the adaxial cells in *fgf3*-/*fgf8*-double-MO-injected embryos (H), it could only be detected in the adaxial cells in embryos treated with SU5402 (I).

The forkhead transcription factor *FoxC1a* plays important roles during early somitogenesis in zebrafish (Topczewska et al., 2001). Therefore, we examined *FoxC1a* to see whether any factor other than *FoxD5* could be the target of Fgf signaling in regulating the striped expression of *mesps*. Interestingly, when *FoxC1a* was knocked down, *mespa* expression remained unchanged (Fig. 7M), whereas *mespb* expression was almost absent (Fig. 7N). We then examined the expression of *FoxC1a* in *fgf3*-/*fgf8*-double-MO-injected embryos and observed that the expression of *FoxC1a* was strongly reduced in the *fgf3*-/*fgf8*-double morphants (Supplementary Fig. S3). Therefore, we proposed that FGF might mediate *FoxC1a*, which is not dependent on *FoxD5*, to control *mesp* gene expression.

Holley et al. (2000) and Oates et al. (2005b) reported that *fss*/*tbx24* may function primarily in a cell-autonomous manner to direct the anterior half-somite fate, which then induces or promotes the adoption of posterior half-somite fate in the neighboring cells. Moreover, in the *tbx24*/*fss* mutant, *mespa*, *mespb, fgf8, notch3* and *papc* almost lost their expressions (Oates et al., 2005b). To more clearly understand the relationship between *tbx24* and *FoxD5* and to distinguish whether *FoxD5* functions in the anterior PSM under the control of *tbx24*, we carried out the rescue experiment of *tbx24* morphants with injection of excessive *FoxD5* mRNA (Fig. 8; Supplementary Table S3). We demonstrated that the somite structure (Fig. 8A) and the striped expression of *myod* (Fig. 8D) were normal in WT embryos. However, in the *tbx24*-MO-injected embryos, the somite structure (Fig. 8B) and the segmental expression of *myod* (Fig. 8E) were lost. Instead, the *myod* transcript was uniformly expressed throughout the somitic region of the paraxial mesoderm (Fig. 8E). When embryos were co-injected with *tbx24*-MO and *FoxD5* mRNA, neither the somitic defect (Fig. 8C) nor the *myod* pattern defect (Fig. 8F) was rescued. In addition, we analyzed the expressions of *mespa* and *mespb* to see whether these somitic polarity genes could be rescued by injection of *FoxD5* mRNA in the *tbx24*-MO-injected embryos. Results showed that the transcripts of *mespa* (82 out of 94 embryos examined; Fig. 8G vs. H) and *mespb* (63 out of 74 embryos examined; Fig. 8K vs. L) in the *tbx24* morphants at 12 hpf were almost lost, a result which is consistent with what Sawada et al. (2000) reported. Surprisingly, we noticed that about 13–15% of *tbx24* morphants still showed uniform expressions of *mespa* (12 out of 94 embryos examined; Fig. 8I) and *mespb* (9 out of 74 embryos examined; Fig. 8M) throughout the anterior PSM region. However, when embryos were co-injected with *tbx24*-MO and *FoxD5* mRNA, all the injected embryos lost *mespa* (Fig. 8J) and *mespb* (Fig. 8N) transcripts during 12 hpf, suggesting that excessive *FoxD5* mRNA

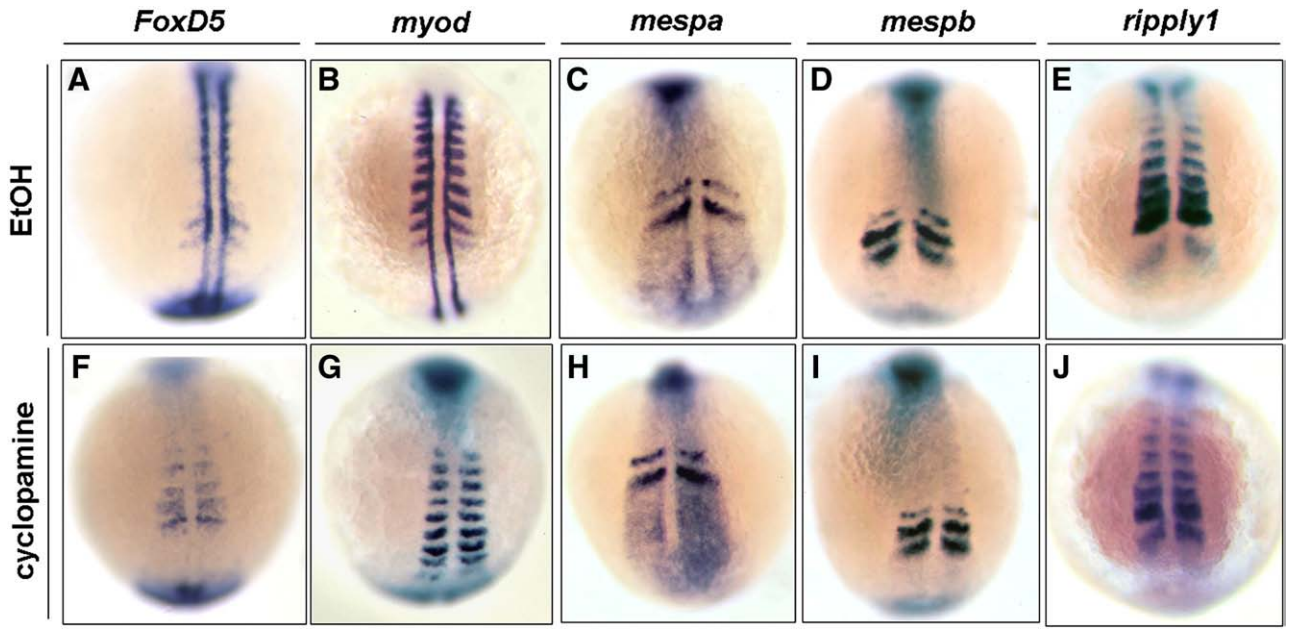

Fig. 6. Hh activity was required for inhibition of *FoxD5* expression in the somites. WISH was used to detect the expression of *FoxD5*, *myod*, *mespa*, *mespb* and *ripply1* in control (EtOH) embryos and cyclopamine-treated embryos, as indicated. Embryos were incubated for 6 h in ethanol (A–E) or cyclopamine (F–J), starting at 6 hpf, followed by WISH analysis at 12 hpf. The expression of *FoxD5* in the adaxial cells was greatly reduced when Hh activity was inhibited (B). Interestingly, a slightly enhanced and extended expression of *FoxD5* in the anterior PSM and somites was observed in cyclopamine-treated embryos (B). In WT embryos, *myod* was detected in the somites and adaxial cells (C). However, although *myod* could still be detected in the somites, it was completely lost in the adaxial cells of cyclopamine-treated embryos (D). Both *mespa* and *mespb* were normally expressed in control embryos (C, D) and cyclopamine-treated embryos (H, I). The repressor *ripply1* was normally detected in control embryos (E) and cyclopamine-treated embryos (J).

did not enable embryos to rescue the defects caused by *tbx24*-MO. Thus, *FoxD5* was not able to induce *mespa* and *mespb* expressions in the absence of *tbx24*.

Discussion

In this study, we investigated a forkhead gene, *FoxD5*, which controls somite morphogenesis. We conclude that (1) the expression of *FoxD5* in the anterior PSM is necessary for anterior–posterior polarity maintenance; (2) Fgf signaling is a major upstream modulator of *FoxD5* expression in the anterior PSM to regulate the anterior–posterior polarity during somite formation; and (3) Fgf-FoxD5-Mesps represents a novel molecular network model for somitogenesis in zebrafish (Fig. 9).

Zebrafish FoxD5 is a downstream target of tbx24 during segmentation

Many studies reveal that *tbx24* is necessary for segmental pre-patterning to initiate the segmentation oscillator in the segment polarity zone (van Eeden et al., 1998; Durbin et al., 2000; Holley et al., 2000; Nikaido et al., 2002; Oates et al., 2005b). In the *tbx24*/*fss* mutant, *mespa*, *mespb, fgf8, notch3* and *papc* nearly lose their expressions (Oates et al., 2005b). In this study, *tbx24* morphants exhibit a normal expression of *FoxD5* in the adaxial cells, but the striped pattern in the anterior PSM is lost (Fig. 4G vs. H). While these findings suggest that *FoxD5* may not be involved in segmental pre-patterning, they do point to *FoxD5* as a possible downstream factor of *tbx24*.

On the other hand, the expression of *tbx24* in the PSM is unaffected in *FoxD5* morphants, while the striped pattern of *tbx24* in somites is disordered (Fig. 4E vs. F). Using the genetic mosaic experiment, Holley et al. (2000) and Oates et al. (2005b) reported that *fss*/*tbx24* may function primarily in a cell-autonomous manner to direct the anterior half-somite fate, which then induces or promotes the adoption of posterior half-somite fate in the neighboring cells. Thus, the remainder of disorganized *tbx24* transcripts in the newly formed somite cells of the *FoxD5* morphants may cause the chaotic expression of some genes, such as *fgf8* (data not shown) and *notch* (Fig. 3) in the neighboring cells. Moreover, the striped pattern of *tbx24* in somites is disordered in *FoxD5* morphants (Fig. 4E vs. F), reveals that there is a feedback control by which *FoxD5* also controls the stripe expression of *tbx24*. Taken together, we proposed that the expression of *FoxD5* is necessary in the *fss*/*tbx24*-expressing cells, whose fates have been determined, and that *FoxD5* controls the somite polarity-associated gene expression, thus completing segmental polarization.

The relationship between muscle differentiation and myotome boundary formation is complex. The *tbx24*/*fss* mutant loses somite structure, but its muscle cell differentiation appears normal (van Eeden et al., 1996; Nikaido et al., 2002), indicating that the somite boundary formation is not dependent on cell differentiation during segmental patterning. However, there are actually two studies indicating that muscle differentiation enables embryos to rescue myotome boundary formation in the segmentation mutant (van Eeden et al., 1998; Henry et al., 2005). In this study, knockdown of *FoxD5* disrupts normal somite boundary formation, but the muscle differentiation is not affected. Although the expression of *myf5* in the somite of *FoxD5*-deficient embryos is lost, other MRFs, such as *myod* and *myogenin*, are still expressed (Supplementary Fig. S4). Moreover, the muscle fibers are detected using MF20 antibody (Supplementary Fig. S5). This line of evidence indicates that the differentiation of anterior PSM cells is processed. We also notice that the striped expressions of *myod* (Fig. S4D; $n=77$, 83%) and *myogenin* (Fig. S4F; $n=94$, 87%) are affected in *FoxD5* morphants. The transcripts of *myod* and *myogenin,* whose signals from the posterior part of somites are extended to the anterior part of somites, are abnormally expressed (Fig. S4). This fact may be a result from the disordered anterior–posterior polarity within the somites of *FoxD5* morphants, which, in turn, accounts for the misalignment of myofibrils (Fig. S5).

FoxD5 functions as an upstream modulator to regulate mespa and mespb differentially during somitogenesis

Zebrafish *mespa* and *mespb* belong to the *Mesp*-related subfamily of bHLH transcription factors, but they are not one-to-one orthologs of

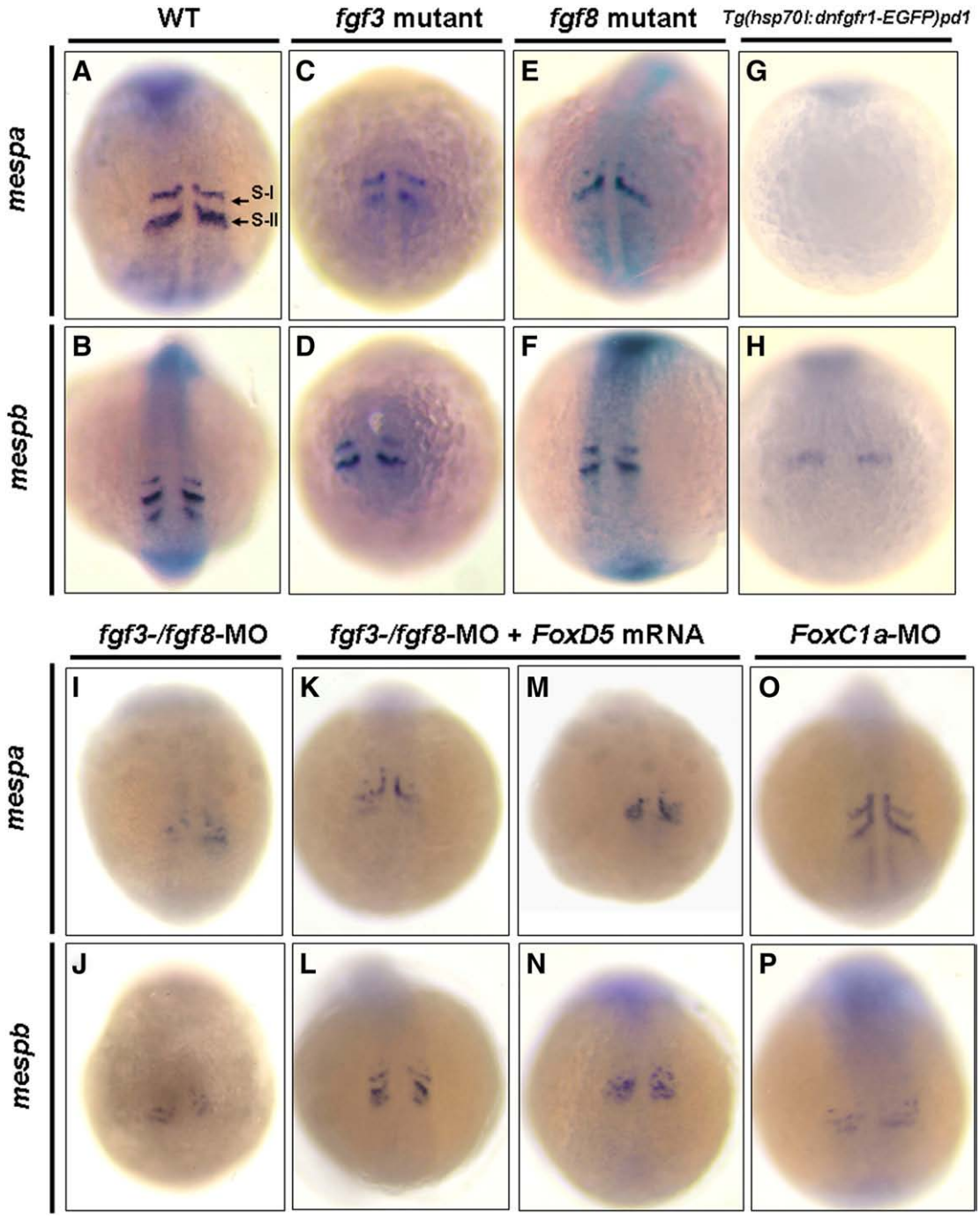

Fig. 7. *FoxD5*, which was mediated by Fgf signaling, controlled *mespa* and *mespb* expressions during somitogenesis. WISH was used to detect *mespa* and *mespb* in the wild-type embryos (WT), mutants and embryos injected with different materials as indicated at 12 hpf. Two stripes of *mespa* expression in the PSM were observable in WT embryos (A), but they were slightly reduced in the *fgf3* mutants (C). The *mespa* signal was lost in S0 in *fgf8* mutants (E) and greatly reduced in the heat-shocked embryos derived from transgenic line *Tg(hsp70l:dnfgfr1-EGFP)pd1* (G) and in the *fgf3*-/*fgf8*-double-MO-injected embryos (I). Three stripes of *mespb* transcripts were detected in the PSM of WT embryos. Although they were slightly reduced in the *fgf3* (D) and *fgf8* mutants (F), these three stripes of *mespb* were greatly lost in the heat-shocked embryos derived from the transgenic line *Tg(hsp70l:dnfgfr1-EGFP)pd1* (H) and in the *fgf3*-/*fgf8*-double-MO-injected embryos (J). Co-injection of *fgf3*-/*fgf8*-double-MO with *FoxD5* mRNA enabled embryos to rescue expression of *mespa* and *mespb*, but neither the striped pattern of *mespa* nor that of *mespb* was restored (K-N). The expression of *mespa* in the *FoxC1a* morphants appeared to be unaffected (O), but the expression of *mespb* in *FoxC1a* morphants was greatly reduced (P).

the murine Mesp1 and Mesp2 gene (Saga et al., 1996 and 1997; Sawada et al., 2000). Mesp1 plays an important role during early cardiac mesoderm lineage specification (Saga et al., 1999; Wu, 2008). However, the role of Mesp1 during somitogenesis is little studied. Mesp2 seems to play major roles in somitogenesis. Mesp2-deficient mice showed a disturbance of the somitic anteroposterior polarity during somitogenesis. Moreover, no paraxial mesoderm is generated in the Mesp1/Mesp2-double-knockout embryo, which results in a complete lack of somites (Saga et al., 2000). Therefore, these two Mesp isoforms are necessary for somite formation.

In zebrafish, gain-of-function studies reveal that ectopic expression of *mespa* causes a severe gastrulation defect, probably caused by the inhibition of mesoderm formation. Ectopic expression of *mespb* causes a loss of the posterior identity within the somite primordium (Sawada et al., 2000). In this report, knockdown of *FoxD5* greatly reduces the *mespa* expression in S-I during somitogenesis, but all

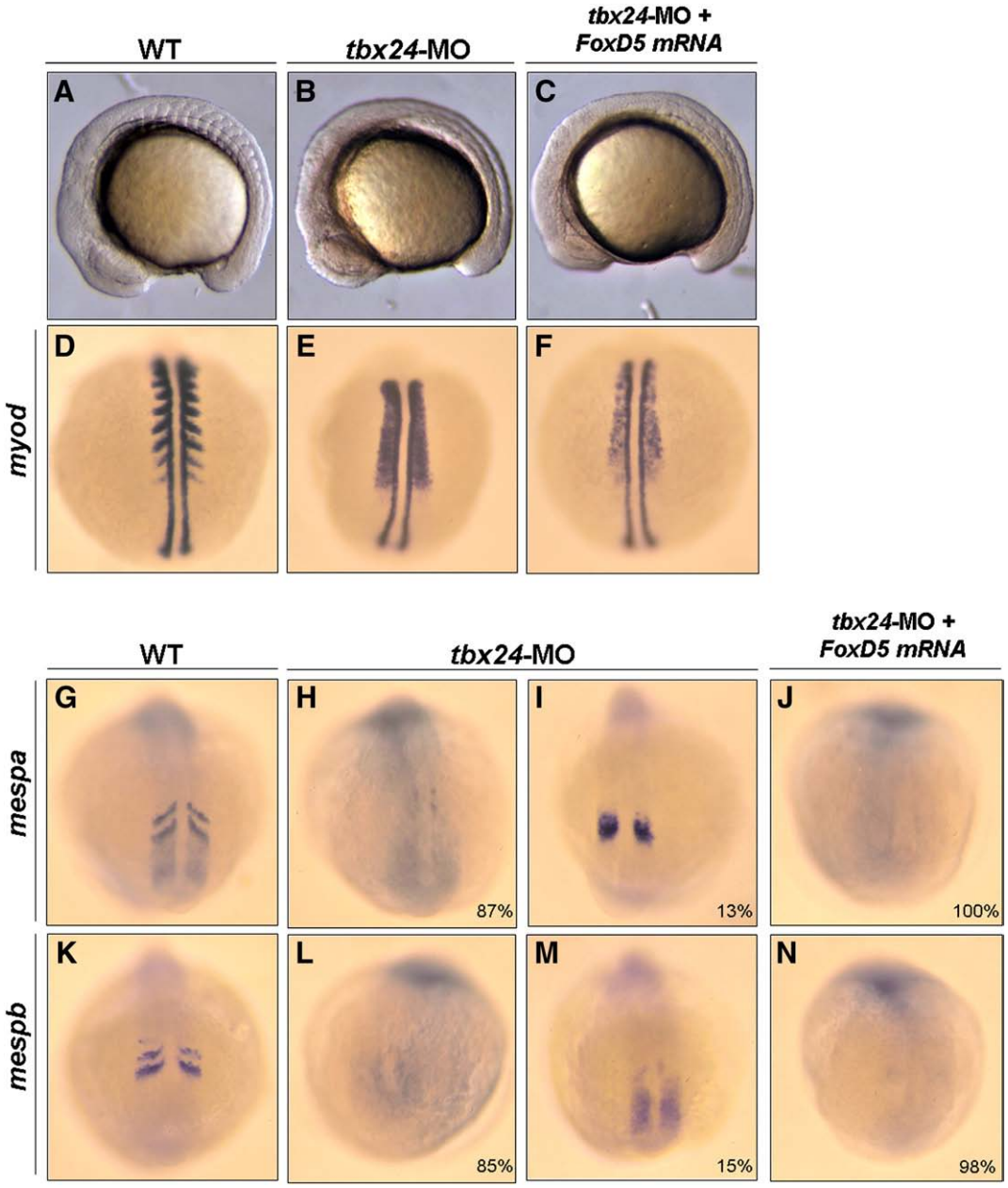

Fig. 8. Excessive *FoxD5* mRNA did not enable embryos to rescue the defects caused by *tbx24*-MO. (A–C) Lateral views of wild-type (WT) and embryos injected with different materials as indicated at 14 hpf. Compared to WT embryos (A), the arrays of the paired somites in *tbx24* morphants (B) were lost. Injection of excessive *FoxD5* mRNA could not rescue the loss of somite structure induced by the knockdown of *tbx24* (C). WISH was performed to detect the expressions of *myod*, *mespa* and *mespb* in WT embryos and in embryos injected with different materials as indicated at 14 hpf. In WT embryos, the segmental expression of *myod* was detected (D). However, in the embryos injected with *tbx24*-MO, the segmental expression of *myod* was lost (E). The defective segmental pattern of *myod* in *tbx24* morphants could not be rescued by injection of *FoxD5* mRNA (F). WT embryos showed striped expressions of *mespa* (G) and *mespb* (K) in the anterior PSM. The segmental expressions of *mespa* (H; $n=89$, 87%) and *mespb* (L; $n=68$, 85%) were totally abolished in *tbx24* morphants. In addition, the scattered expressions of *mespa* (I; $n=89$, 13%) and *mespb* (M; $n=68$, 15%) were also observed in the anterior PSM of *tbx24* morphants. Injection of excessive *FoxD5* mRNA did not enable embryos to rescue either the striped pattern or the expression levels of *mespa* (J; $n=47$, 100%) and *mespb* (N; $n=53$, 98%) in the *tbx24* morphants.

FoxD5 morphants exhibit normal *mespa* expression during gastrulation, suggesting that *mespa* and *FoxD5* play out their roles in different pathways during gastrulation. Specifically, our data demonstrated a differential requirement of FoxD5 protein for expressions of *mespa* and *mespb*. While the expression of *mespa* is greatly reduced in *FoxD5*-knockdown embryos in S-I (Fig. 4B), the expression of *mespb* loses its striped pattern and shows a "salt and pepper" pattern (Fig. 4D). In other mutants, such as *bea*, *des*, *aei* and *mib*, the *mespb* expression pattern shows a mosaic "salt and pepper" pattern. Here, we notice that the "salt and pepper" pattern of *mespb* expression in *FoxD5* morphants is not as disorganized as seen in the *Notch* mutants, suggesting that the factor causing the "salt and pepper" pattern of *mespb* expression in *FoxD5* morphants may not be the same as that affecting *Notch* mutants. On the other hand, *mespa* expression in these mutants tends to be very weak and slightly diffuse, which is different from that of *FoxD5* morphants which only lost *mespa* expression in S-I (Fig. 4; Sawada et al., 2000). We therefore proposed that *FoxD5* directs *mespa* expression in S-I and that the disordered expression of *mespb* probably results from an indirect effect caused by irregular segmentation. This evidence also reveals that *mespa* and *mespb* are differentially regulated. The same differential effect on *mesp* expression has also been observed in *FoxC1a* morphants

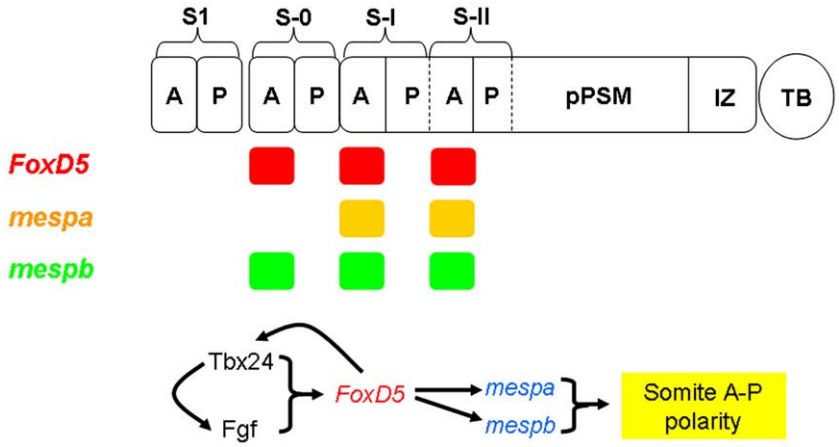

Fig. 9. A plausible model representing the modulation of *FoxD5* during somitogenesis in zebrafish. Schematic illustration of a signaling network model for somitogenesis in zebrafish embryos. Regulated by Tbx24 and Fgf signaling, *FoxD5*, which is confirmatively expressed in the anterior PSM, ultimately controls the differential expressions of *mesps* which, in turn, regulate somite polarity. *FoxD5* also inhibits *papc* and maintains the striped pattern of *paraxis* to control the MET processes during somite formation.

(Topczewska et al., 2001) and *ripply1* morphants (Kawamura et al., 2005a).

Interestingly, in our study, knockdown of either *mespa* or *mespb* in zebrafish causes a defect in somite boundary formation (Supplementary Table S1;Fig. S6), indicating the importance of *mesps* in somite formation. We also show that *mesps* do not represent upstream modulators of *FoxD5*, particularly since normal expression of *FoxD5* is observed in *mespa* and *mespb* morphants (Fig. S6).

The role of FoxD5 in the anterior PSM is to maintain the anterior–posterior polarity identity

The Notch signaling pathway is critically necessary for somite development. Mesp2 plays important roles in somite anterior–posterior patterning through interaction with Notch/Delta signaling (Takahashi et al. 2000). We concluded that the activities of both *mespa* and *mespb* are required for guiding the anterior–posterior patterning of the presumptive somites and that the defects in the anterior PSM are accompanied by the absence of the striped expression of *notch2* and *notch3* genes in the mature somites of *FoxD5* morphants (Fig. 3). We noticed that the expression level of *deltaC* is greatly reduced in the somites of *FoxD5* morphants (Fig. 3C vs. D). The decrease of *deltaC* may result in abnormal segmental patterns of *notch2* and *notch3* in the somites, which are similar to those of the phenotypes induced by *deltaC*-MO, as reported by Oates et al. (2005a). Thus, *FoxD5* is necessary for the normal patterns of *mesp* and *notch* genes, indicating that the role of *FoxD5* involves anterior–posterior patterning. Although the *Notch* gene in the somite is affected when *FoxD5* is knocked down, the oscillation of the *Notch* gene in the PSM is normal. Moreover, by measuring the length between the tailbud and anterior PSM of embryos co-injected with *fgf3*-/*fgf8*-double-MO and *FoxD5* mRNA, we find that excessive *FoxD5* mRNA enables embryos to rescue the defective expression of *mesp*, but it does not enable rescue of either gene expression in the posterior PSM or the maturation state of the PSM (data not shown). Taken together, we proposed that the absence of FoxD5 protein does not influence the oscillation of cells in the PSM.

On the other hand, our data demonstrate that excessive *FoxD5* mRNA can enhance *mesp* gene expression only in the anterior PSM of the *fgf3*-/*fgf8*-MO-injected embryos, even though the injected *FoxD5* mRNA is distributed ubiquitously. Moreover, our data also show that excessive *FoxD5* mRNA does not enable rescue of the decreased expression of *mesp* genes induced by the knockdown of *tbx24* (Fig. 8). These evidence indicate that *FoxD5* is not able to induce either *mespa* or *mespb* expression in the absence of *tbx24.* Many studies have proven that *tbx24* is primarily cell-autonomous to direct the anterior half-somite fate, which then induces or promotes the adoption of posterior fates in neighboring cells (Holley et al., 2000; Oates et al., 2005b; Holley, 2007). Based on this evidence, we proposed the existence of an *fss*/*tbx24*-dependent, cell–cell signaling in the anterior PSM which helps *FoxD5* induce the expression of *mespa* and *mespb*. *FoxD5* is not able to activate *mesp* genes alone, suggesting that *FoxD5* is required for the maintenance of *mesp* expression.

Fgf-FoxD5-Mesps signaling network controls somite formation

During somite formation, Fgf signaling plays important roles in regulating the differentiation of PSM cells along the anterior–posterior axis from a state which permits oscillating gene expression to a state which drives the segmentation processes. Specifically, while intensity gradients of Fgf signaling in the PSM maintain cells of the posterior PSM in an immature state, these same signaling gradients also control the maturation wavefront in anterior PSM (Goldbeter and Pourquié, 2008). MET is also controlled by the level of FGF signaling in the PSM, and the MET process begins once the cells enter the anterior PSM, which is characterized by lower Fgf signaling (Dubrulle et al., 2001; Delfini et al., 2005). In the anterior PSM of chick and mouse embryos, the beginning of the epithelialization process correlates with the down-regulation of Snail1 and Snail2 and is mediated by Fgf signaling (Sefton et al., 1998; Dale et al. 2006). Therefore, Fgf signaling is not only involved in oscillating gene expression in the PSM, but also the MET process during somite formation. Moreover, no matter whether we inhibit FGFR or knock down Fgf ligands, the expression of *FoxD5* is inhibited significantly, suggesting that Fgf signaling directs *FoxD5* expression during somitogenesis. Additionally, both double knockdown of *fgf3*/*fgf8* and inhibition of FGFR cause the loss of almost all the *FoxD5* transcripts. These results indicate that Fgf factors might play a redundant function in mediating *FoxD5* expression. Our data also demonstrated that Fgf signaling is necessary for the expression of *mespa* and *mespb*. Therefore, we propose a *de novo* Fgf-FoxD5-Mesps signaling cascade during somitogenesis.

Although the expression levels of *mespa* and *mespb* are greatly rescued by *FoxD5* mRNA in the *fgf3*-/*fgf8*-double-MO-injected embryos, we notice again that the striped patterns of *mespa* and *mespb* are not restored in the absence of Fgf signaling. Furthermore, *FoxC1a* is strongly reduced in the *fgf3*-/*fgf8*-double-MO-injected embryos (Supplementary Fig. S3). Knockdown of FoxC1a loses the expression of *mespb* during early somitogenesis (Fig. 7P). Moreover, Wahl et al. (2007) proved that Fgf acts upstream of the Wnt and Notch pathways to control the segmentation clock oscillations. Therefore, it

is plausible that Fgf might mediate the Wnt and Notch pathways, which are independent of *FoxD5*, to control somite formation. This evidence indicates that the entire Fgf-mediated regulatory network during somite formation is a complex process, which leads to the speculation that Fgf might regulate somite formation in a multi-signaling manner, not exclusively through *FoxD5*.

Another possibility is that the ubiquitous, but not stripy, expression of *FoxD5* mRNA in *fgf3*-/*fgf8*-double morphants might explain why injection of *FoxD5* mRNA does not help at all to recover the stripy expression of the *mesps* genes. That is, the expression of *mesps* genes cannot be completely rescued by providing *FoxD5* mRNA everywhere in the *fgf3*-/*fgf8*-double morphants.

The expression of FoxD5 in the anterior PSM is confirmed by Hh signaling

Hh signaling plays important roles during somitogenesis (Borello et al., 2006). When cyclopamine interferes with Hh signaling, development of adaxial cells is inhibited (Fig. 7). Interestingly, the ectopic expression of *FoxD5* in the anterior PSM and the extension of striped pattern from S-2 to S-4 are observed in Hh-deficient embryos. These results suggest that Hh signaling is necessary to confine *FoxD5* expression to the anterior PSM. Although the *FoxD5* transcripts are ectopically expressed in somites, neither *mespa* nor *mespb* is extended into somites. This might result from the fact that the repressor *ripply1* is still present in the somites of *FoxD5* morphants, which results in confinement of the expressions of *mespa* and *mespb* in somites (Fig. 6J). Additionally, although most genes that are expressed in anterior PSM and involved in somite segmentation are repressed by *ripply1*, these results also reveal that *FoxD5* is not repressed by *ripply1* (Kawamura et al., 2005a).

Acknowledgments

We thank S. Wilson, E. de Robertis and S. Takada for providing the probes of zebrafish *her1 intron, paraxis, papc, ripply1*, *notch2,* and *notch3*. We also thank Yi-Hua Chiu, Instrument Center of Taipei Medical University, for operating the confocal microscope. This work was supported by the National Science Council, Republic of China, under grant number NSC98-2321-B-002-024. This project is also sponsored by the National Health Research Institute of Taiwan under NHRI-EX98-9201EI and by the National Taiwan University Research Center for Medical Excellence.

Appendix A. Supplementary data

Supplementary data associated with this article can be found, in the online version, at doi:10.1016/j.ydbio.2009.10.001.

References

Borello, U., Berarducci, B., Murphy, P., Bajard, L., Buffa, V., Piccolo, S., Buckingham, M., Cossu, G., 2006. The Wnt/beta-catenin pathway regulates Gli-mediated Myf5 expression during somitogenesis. Development 133, 3723–3732.

Burgess, R., Cserjesi, P., Ligon, K.L., Olson, E.N., 1995. Paraxis: a basic helix–loop–helix protein expressed in paraxial mesoderm and developing somites. Dev. Biol. 168, 296–306.

Burgess, R., Rawls, A., Brown, D., Bradley, A., Olson, E.N., 1996. Requirement of the paraxis gene for somite formation and musculoskeletal patterning. Nature 384, 570–573.

Cooke, J., Zeeman, E.C., 1976. A clock and wavefront model for control of the number of repeated structures during animal morphogenesis. J. Theor. Biol. 58, 455–476.

Cooper, M.K., Porter, J.A., Young, K.E., Beachy, P.A., 1998. Teratogen-mediated inhibition of target tissue response to Shh signaling. Science 280, 1603–1607.

Dale, J.K., Malapert, P., Chal, J., Vilhais-Neto, G., Maroto, M., Johnson, T., Jayasinghe, S., Trainor, P., Herrmann, B., Pourquié, O., 2006. Oscillations of the snail genes in the presomitic mesoderm coordinate segmental patterning and morphogenesis in vertebrate somitogenesis. Dev. Cell 10, 355–366.

Delfini, M.C., Dubrulle, J., Malapert, P., Chal, J., Pourquié, O., 2005. Control of the segmentation process by graded MAPK/ERK activation in the chick embryo. Proc. Natl. Acad. Sci. U. S. A. 102, 11343–11348.

Dubrulle, J., Pourquié, O., 2004. Coupling segmentation to axis formation. Development 131, 5783–5793.

Dubrulle, J., McGrew, M.J., Pourquié, O., 2001. FGF signaling controls somite boundary position and regulates segmentation clock control of spatiotemporal *Hox* gene activation. Cell 106, 219–232.

Durbin, L., Brennan, C., Shiomi, K., Cooke, J., Barrios, A., Shanmugalingam, S., Guthrie, B., Lindberg, R., Holder, N., 1998. Eph signaling is required for segmentation and differentiation of the somites. Genes Dev. 121, 3096–3109.

Durbin, L., Sordino, P., Barrios, A., Gering, M., Thisse, C., Thisse, B., Brennan, C., Green, A., Wilson, S., Holder, N., 2000. Anteroposterior patterning is required within segments for somite boundary formation in developing zebrafish. Development 127, 1703–1713.

Gajewski, M., Sieger, D., Alt, B., Leve, C., Hans, S., Wolff, C., Rohr, K.B., Tautz, D., 2003. Anterior and posterior waves of cyclic *her1* gene expression are differentially regulated in the presomitic mesoderm of zebrafish. Development 130, 4269–4278.

Garry, D.J., Meeson, A., Elterman, J., Zhao, Y., Yang, P., Bassel-Duby, R., Williams, R.S., 2000. Myogenic stem cell function is impaired in mice lacking the forkhead/winged helix protein MNF. Proc. Natl. Acad. Sci. U.S.A. 97, 5416–5421.

Goldbeter, A., Pourquié, O., 2008. Modeling the segmentation clock as a network of coupled oscillations in the Notch, Wnt and FGF signaling pathways. J. Theor. Biol. 252, 574–585.

Hart, D.O., Raha, T., Lawson, N.D., Green, M.R., 2007. Initiation of zebrafish haematopoiesis by the TATA-box-binding protein-related factor Trf3. Nature 450, 1082–1085.

Hatini, V., Huh, S.O., Herzlinger, D., Soares, V.C., Lai, E., 1996. Essential role of stromal mesenchyme in kidney morphogenesis revealed by targeted disruption of Winged Helix transcription factor BF-2. Genes Dev. 10, 1467–1478.

Henry, C.A., McNulty, I.M., Durst, W.A., Munchel, S.E., Amacher, S.L., 2005. Interactions between muscle fibers and segment boundaries in zebrafish. Dev. Biol. 287, 346–360.

Herzog, W., Sonntag, C., von der Hardt, S., Roehl, H.H., Varga, Z.M., Hammerschmidt, M., 2004. Fgf3 signaling from the ventral diencephalon is required for early specification and subsequent survival of the zebrafish adenohypophysis. Development 131, 3681–3692.

Holley, S.A., 2007. The genetics and embryology of zebrafish metamerism. Dev. Dyn. 236, 1422–1449.

Holley, S.A., Geisler, R., Nüsslein-Volhard, C., 2000. Control of *her1* expression during zebrafish somitogenesis by a delta-dependent oscillator and an independent wave-front activity. Genes Dev. 14, 1678–1690.

Ingham, P.W., McMahon, A.P., 2001. Hedgehog signaling in animal development: paradigms and principles. Genes Dev. 15, 3059–3087.

Jiang, Y.J., Aerne, B.L., Smithers, L., Haddon, C., Ish-Horowicz, D., Lewis, J., 2000. Notch signalling and the synchronization of the somite segmentation clock. Nature 408, 475–479.

Johnson, J., Rhee, J., Parsons, S.M., Brown, D., Olson, E.N., Rawls, A., 2000. The anterior/posterior polarity of somites is disrupted in paraxis-deficient mice. Dev. Biol. 229, 1–12.

Kaestner, K.H., Knochel, W., Martinez, D.E., 2000. Unified nomenclature for the winged helix/forkhead transcription factors. Genes Dev. 14, 142–146.

Kalinichenko, V.V., Lim, L., Stolz, D.B., Shin, B., Rausa, F.M., Clark, J., Whitsett, J.A., Watkins, S.C., Costa, R.H., 2001. Defects in pulmonary vasculature and perinatal lung hemorrhage in mice heterozygous null for the Forkhead Box F1 transcription factor. Dev. Biol. 235, 489–506.

Kawamura, A., Koshida, S., Hijikata, H., Ohbayashi, A., Kondoh, H., Takada, S., 2005a. Groucho-associated transcriptional repressor ripply1 is required for proper transition from the presomitic mesoderm to somites. Dev. Cell 9, 735–744.

Kawamura, A., Koshida, S., Hijikata, H., Sakaguchi, T., Kondoh, H., Takada, S., 2005b. Zebrafish hairy/enhancer of split protein links FGF signaling to cyclic gene expression in the periodic segmentation of somites. Genes Dev. 19, 1156–1161.

Kimelman, D., 2006. Mesoderm induction: From caps to chips. Nat. Rev. Genet. 7, 360–372.

Lee, Y., Grill, S., Sanchez, A., Murphy-Ryan, M., Poss, K.D., 2005. Fgf signaling instructs position-dependent growth rate during zebrafish fin regeneration. Development 132, 5173–5183.

Lee, H.C., Huang, H.Y., Lin, C.Y., Che n, Y.H., Tsai, H.J., 2006. Foxd3 mediates zebrafish myf5 expression during early somitogenesis. Dev. Biol. 290, 359–372.

Mohammadi, M., McMahon, G., Sun, L., Tang, C., Hirth, P., Yeh, B.K., Hubbard, S.R., Schlessinger, J., 1997. Structures of the tyrosine kinase domain of fibroblast growth factor receptor in complex with inhibitors. Science 276, 955–960.

Nikaido, M., Kawakami, A., Sawada, A., Furutani-Seiki, M., Takeda, H., Araki, K., 2002. Tbx24, encoding a T-box protein, is mutated in the zebrafish somite-segmentation mutant fused somites. Nat. Genet. 31, 195–199.

Oates, A.C., Mueller, C., Ho, R.K., 2005a. Cooperative function of deltaC and her7 in anterior segment formation. Dev. Biol. 280, 133–149.

Oates, A.C., Rohde, L.A., Ho, R.K., 2005b. Generation of segment polarity in the paraxial mesoderm of the zebrafish through a T-box-dependent inductive event. Dev. Biol. 283, 204–214.

Odenthal, J., Nüsslein-Volhard, C., 1998. fork head domain genes in zebrafish. Dev Genes Evol. 208, 245–258.

Ozbudak, E.M., Pourquié, O., 2008. The vertebrate segmentation clock: the tip of the iceberg. Curr. Opin. Genet. Dev. 18, 317–323.

Phillips, B.T., Bolding, K., Riley, B.B., 2001. Zebrafish fgf3 and fgf8 encode redundant functions required for otic placode induction. Dev. Biol. 235, 351–365.

Raible, F., Brand, M., 2001. Tight transcriptional control of the ETS domain factors Erm and Pea3 by Fgf signaling during early zebrafish development. Mech. Dev. 107, 105–117.

Roehl, H., Nüsslein-Volhard, C., 2001. Zebrafish pea3 and erm are general targets of FGF8 signaling. Curr. Biol. 11, 503–507.
Saga, Y., Hata, N., Kobayashi, S., Magnuson, T., Seldin, M.F., Taketo, M.M., 1996. MesP1: a novel basic helix–loop–helix protein expressed in the nascent mesodermal cells during mouse gastrulation. Development 122, 2769–2778.
Saga, Y., Hata, N., Koseki, H., Taketo, M.M., 1997. Mesp2: a novel mouse gene expressed in the presegmented mesoderm and essential for segmentation initiation. Genes Dev. 11, 1827–1839.
Saga, Y., Miyagawa-Tomita, S., Takagi, A., Kitajima, S., Miyazaki, J., Inoue, T., 1999. MesP1 is expressed in the heart precursor cells and required for the formation of a single heart tube. Development 126, 3437–3447.
Saga, Y., Kitajima, S., Miyagawa-Tomita, S., 2000. Mesp1 expression is the earliest sign of cardiovascular development. Trends Cardiovasc. Med. 10, 345–352.
Sawada, A., Fritz, A., Jiang, Y.-J., Yamamoto, A., Yamasu, K., Kuroiwa, A., Saga, Y., Takeda, H., 2000. Zebrafish Mesp family genes, mesp-a and mesp-b are segmentally expressed in the presomitic mesoderm, and Mesp-b confers the anterior identity to the developing somites. Development 127, 1691–1702.
Sawada, A., Shinya, M., Jiang, Y.J., Kawakami, A., Kuroiwa, A., Takeda, H., 2001. Fgf/MAPK signalling is a crucial positional cue in somite boundary formation. Development 128, 4873–4880.
Sefton, M., Sanchez, S., Nieto, M.A., 1998. Conserved and divergent roles for members of the Snail family of transcription factors in the chick and mouse embryo. Development 125, 3111–3121.
Sun, C.K., Chu, S.W., Chen, S.Y., Tsai, T.H., Liu, T.M., Lin, C.Y., Tsai, H.J., 2004. Higher harmonic generation microscopy for developmental biology. J. Struct. Biol. 147, 19–30.
Takahashi, Y., Koizumi, K., Takagi, A., Kitajima, S., Inoue, T., Koseki, H., Saga, Y., 2000. Mesp2 initiates somite segmentation through the Notch signalling pathway. Nat. Genet. 25, 390–396.
Takke, C., Campos-Ortega, J.A., 1999. her1, a zebrafish pairrule gene, acts downstream of Notch signaling to control somite development. Development 126, 3005–3014.
Topczewska, J.M., Topczewski, J., Shostak, A., Kume, T., Solnica-Krezel, L., Hoga n, B.L.M., 2001. The winged helix transcription factor FoxC1a is essential for somitogenesis in zebrafish. Genes Dev. 15, 2483–2493.
van Eeden, F.J., Granato, M., Schach, U., Brand, M., Furutani-Seiki, M., Haffter, P., Hammerschmidt, M., Heisenberg, C.P., Jiang, Y.J., Kane, D.A., Kelsh, R.N., Mullins, M.C., Odenthal, J., Warga, R.M., Allende, M.L., Weinberg, E.S., Nüsslein-Volhard, C., 1996. Mutations affecting somite formation and patterning in the zebrafish *Danio rerio*. Development 123, 153–164.
van Eeden, F.J., Holley, S.A., Haffter, P., Nüsslein-Volhard, C., 1998. Zebrafish segmentation and pair-rule patterning. Dev. Genet. 23, 65–76.
Wahl, M.B., Deng, C., Lewandoski, M., Pourquié, O., 2007. FGF signaling acts upstream of the NOTCH and WNT signaling pathways to control segmentation clock oscillations in mouse somitogenesis. Development 134, 4033–4041.
Weinstein, D.C., Ruiz i Altaba, A., Chen, W.S., Hoodless, P., Prezioso, V.R., Jessell, T.M., Darnell, J.E., 1994. The winged-helix transcription factor HNF-3b is required for notochord development in the mouse embryo. Cell 78, 575–588.
Westerfield, M., 1995. The zebrafish book, 3rd ed. University of Oregon Press, Eugene, OR.
Westerfield, M., 2000. The Zebrafish Book:AGuide for the Laboratory Use of Zebrafish (Brachydanio rerio). University of Oregon Press, Eugene, OR.
Wijcher s, P.J., Burbach, J.P., Smidt, M.P., 2006. In control of biology: of mice, men and Foxes. Biochem. J. 397, 233–246.
Wilm, B., James, R.G., Schultheiss, T.M., Hogan, B.L., 2004. The forkhead genes, Foxc1 and Foxc2, regulate paraxial versus intermediate mesoderm cell fate. Dev. Biol. 271, 176–189.
Wu, S.M., 2008. Mesp1 at the heart of mesoderm lineage specification. Cell Stem Cell 3, 1–2.
Yamamoto, A., Amacher, S.L., Kim, S.H., Geissert, D., Kimmel, C.B., De Robertis, E.M., 1998. Zebrafish paraxial protocadherin is a downstream target of spadetail involved in morphogenesis of gastrula mesoderm. Development 125, 3389–3397.